Origin of basal activity in mammalian olfactory receptor neurons

Johannes Reisert

Monell Chemical Senses Center, Philadelphia, PA 19104

Mammalian odorant receptors form a large, diverse group of G protein–coupled receptors that determine the sensitivity and response profile of olfactory receptor neurons. But little is known if odorant receptors control basal and also stimulus-induced cellular properties of olfactory receptor neurons other than ligand specificity. This study demonstrates that different odorant receptors have varying degrees of basal activity, which drives concomitant receptor current fluctuations and basal action potential firing. This basal activity can be suppressed by odorants functioning as inverse agonists. Furthermore, odorant-stimulated olfactory receptor neurons expressing different odorant receptors can have strikingly different response patterns in the later phases of prolonged stimulation. Thus, the influence of odorant receptor choice on response characteristics is much more complex than previously thought, which has important consequences on odor coding and odor information transfer to the brain.

INTRODUCTION

Mammalian odorant receptors (ORs) are a large group of G protein–coupled receptors (GPCRs) that comprise $\sim$1,000 functional receptors in rodents and 350 in humans (Mombaerts, 2004; Malnic, 2007; Spehr and Munger, 2009) and function in at least two roles. First, ORs located on the cilia of olfactory receptor neurons (ORNs) convey odorant specificity and sensitivity, with a given ORN thought to only express one OR type. Considerable progress has been made in de-orphaning odorant receptors since the first odorant–ligand pair, octanal and the I7 receptor, was identified (Zhao et al., 1998), and main aspects of olfactory transduction are relatively well understood. Activation of ORs increases, via the G protein G_{olf}, adenylyl cyclase III (ACIII) activity and ciliary cAMP levels. Na^+ and Ca^{2+} influx ensues through the olfactory CNG channel, and the elevated Ca^{2+} gates a second ion channel, the excitatory Ca^{2+}-activated Cl^- channel Ano2 (Kleene, 1993; Stephan et al., 2009), which carries up to 80% of the overall transduction current (Kurahashi and Yau, 1993; Lowe and Gold, 1993; Reisert et al., 2005). To terminate the response, cAMP is degraded to AMP by the phosphodiesterase PDE1C (Cygnar and Zhao, 2009) and Ca^{2+} is removed in mouse ORNs from the cilia by a Na^+/Ca^{2+} exchanger (Reisert and Matthews, 2001a) to close the CNG channel and Ca^{2+}-activated Cl^- channel, respectively. (For a review of the cAMP pathway of olfactory transduction and other signal transduction pathways present in cells in the olfactory epithelium see Kleene, 2008; Fleischer et al., 2009; Kato and Touhara, 2009; Munger et al.,

2009; Kaupp, 2010). In the absence of stimulation, individual ORNs typically show low spontaneous action potential (AP) firing rates ranging from 0 to 3 Hz (O'Connell and Mozell, 1969; Trotier and MacLeod, 1983; Frings et al., 1991; Reisert and Matthews, 2001b). The origin of this variation in basal activity is unknown but ORNs have been found to be intrinsically noisy, displaying variation in baseline current in the absence of odorants (Lowe and Gold, 1995).

Odorant receptors have a second important function in ORN axon targeting (Mombaerts, 2006; Imai and Sakano, 2008; Zou et al., 2009). Axons of ORNs expressing a given OR coalesce and converge on typically two glomeruli per bulb, with ORs thought to play an instructive role. Recently, ACIII and the G protein $G_{\alpha s}$, which is expressed in immature ORNs unlike $G_{\alpha olf}$, have been implicated in contributing to glomerular map formation. Constitutively active forms of $G_{\alpha s}$ can lead to the formation of ectopic glomeruli and a posterior shift of glomeruli in the bulb (Imai et al., 2006; Chesler et al., 2007).

Besides providing odorant specificity to ORNs and contributing to targeting ORN axons, mammalian OR contribution to olfactory response properties is not understood. For example, do they determine response pattern and basal activity, as do *Drosophila* (ligand-gated) ORs (for review see Dahanukar et al., 2005; Su et al., 2009)? I investigated response characteristics of mouse ORNs expressing identified ORs with known ligands and demonstrate that different ORs display different constitutive activity. In the absence of odorant stimulation and depending on OR choice, ORNs display varying

Correspondence to Johannes Reisert: jreisert@monell.org

Abbreviations used in this paper: ACIII, adenylyl cyclase III; AP, action potential; chca, cycloheptanecarbaldehyde; GPCR, G protein–coupled receptor; IBMX, 3-isobutyl-1-methylxanthine; OR, odorant receptor; ORN, olfactory receptor neuron.

The Rockefeller University Press $30.00
J. Gen. Physiol. Vol. 136 No. 5   529–540
www.jgp.org/cgi/doi/10.1085/jgp.201010528

529

levels of basal transduction activity and current fluctuations (noise) that drive concomitant AP firing. The latter can be suppressed by odorants that function as inverse agonists, suggesting a new mechanism to mediate inhibitory odorant responses. Additionally, ORs determine the response patterns of ORNs during prolonged stimulation. These findings also suggest how ORs can contribute to the targeting of ORN axons to their glomeruli in the olfactory bulb, which is dependent on properties of the expressed OR.

MATERIALS AND METHODS

Electrophysiological recordings
Adult mice were euthanized using CO_2 followed by decapitation as approved by the Monell Chemical Senses Center Institutional Animal Care and Use Committee, conforming to National Institutes of Health guidelines. Olfactory turbinates were removed from the nasal cavity and stored in oxygenated Ringer's solution at 4°C until use. A small piece of olfactory epithelium was freed from the underlying cartilage, placed in an Eppendorf tube containing 200 μl Ringer's solution and briefly vortexed (Reisert and Matthews, 2001a). The resulting cell suspension containing isolated ORNs was transferred to a recording chamber on an inverted microscope equipped with phase-contrast optics, and was allowed to settle for 20 min before bath perfusion began. GFP-positive ORNs were identified with fluorescent optics.

The suction pipette technique was used to record from ORNs (Lowe and Gold, 1991; Reisert and Matthews, 2001a). The cell body of an isolated mouse ORN was drawn into the tip of the recording pipette, leaving the cilia exposed to the bath solution and accessible to solution changes. In this recording configuration, the recorded current represents the transduction current that enters at the cilia and exits at the cell body. In addition, since the intracellular voltage is free to vary, ORNs can generate APs, which were also recorded as typically biphasic, fast current transients. The suction pipette current was filtered at DC-5000 Hz (-3dB, 8-pole Bessel filter) to record the fast APs, and DC-50 Hz to only record the slower receptor current. The sampling rate was 10 kHz. Currents were recorded with a Warner PC-501A patch clamp amplifier, digitized using a Mikro1401 A/D converter and Signal acquisition software (Cambridge Electronic Design).

Not all GFP-positive ORNs obtained from the three mouse lines used responded to their respective ligands, and the percentage of responsive ORNs varied between 35% (M71-GFP and mOR-EG-GFP mouse lines) and 73% (I7-GFP line). This was probably not caused by spurious expression of GFP in cells other than ORNs expressing the tagged receptor, but rather was due to loss of cilia, caused by the isolation procedure. Grosmaitre et al. (2006) used a whole-epithelium approach to electrophysiologically study ORNs expressing the odorant receptor mOR23 (ligand lyral). They reported that 100% of mOR23-positive ORNs responded to lyral, indicating that in their whole-epithelium preparation, ORNs seemed to remain healthier.

Fast solution changes and odorant exposures were achieved by transferring the tip of the recording pipette containing the ORN across the interface of neighboring streams of solutions using the Perfusion Fast-Step solution changer (Warner Instrument Corporation). Solution exchange was complete within 7 ms, as determined from the 10–90% rise or fall time of a junction current, which was elicited by stepping between solutions of different ionic content. All experiments were performed at mammalian body temperature (37°C). Solutions were heated just before entering the solution changer by a solution heater based on Matthews (1999).

Mammalian Ringer's solution contained (in mM) 140 NaCl, 5 KCl, 1 $MgCl_2$, 2 $CaCl_2$, 0.01 EDTA, 10 HEPES, and 10 glucose. The pH was adjusted to 7.5 with NaOH. Cineole solutions were made from a 1 mM stock. Heptanal, cycloheptanecarbaldehyde, acetophenone, and eugenol solutions were prepared daily from a 20 mM DMSO stock. Niflumic acid and 3-isobutyl-1-methylxanthine (IBMX) were used at concentrations of 300 μM and 1 mM, respectively, by dissolving them directly into Ringer's without the use of DMSO. All chemicals were purchased from Sigma-Aldrich, with the exception of cycloheptanecarbaldehyde, which was obtained from ABCR.

Data analysis
The basal firing rate was determined from 30-s recordings taken in the beginning after establishing the recording configuration. Typically the ORN had only been exposed to a single, 1-s exposure of its respective ligand to avoid possible adaptation effects. All APs over the 30-s period were counted, and this number was divided by 30 s to obtain the mean basal spike frequency.

The frequency composition in the absence of stimulation and in the presence of niflumic acid was evaluated by performing power spectra analysis on single 30-s recordings (Fig. 1, trace 0–30 and 30–60 s, respectively, DC-5000 Hz) using Origin and Clampfit Software. Power spectra for impulse responses were performed on 10 sweeps of 1-s duration, and power spectra were subsequently averaged.

The variance of baseline recordings was determined as follows. The variance of the recording in the presence of niflumic acid (Fig. 1, trace 30–60 s) was subtracted from the variance in the absence of niflumic acid (Fig. 1, trace 0–30 s), yielding the current variance carried by the Ca^{2+}-activated Cl^- conductance (Figs. 2 and 4, ΔVar). Before calculating the variance, current recordings were high-pass filtered at 0.3 Hz to exclude slow baseline drifts in the variance. Baseline drifts are difficult to avoid because of the low resistance of the recording configuration and the slightly changing solution level in the recording chamber. Also, current recordings were low-pass Bessel filtered at 50 Hz to only include variance in the frequency band relevant for the transduction current.

The response patterns during long (typically 8 s) odor stimulations were evaluated by autocorrelating the suction pipette current (bandwidth DC-50 Hz). The first second of the response was excluded from the autocorrelation to exclude the larger initial response at the onset of stimulation from the autocorrelation.

RESULTS

The odorant receptor, transduction noise, and basal action potential firing
Odorant receptor–specific contributions to ORN properties were investigated by recording from ORNs from three mouse lines that expressed GFP with the mOR-EG, the I7, or the M71 odorant receptor. The GFP-labeled I7 and M71 mouse lines were generated by inserting IRES-tauGFP after the mouse I7 and M71 coding sequences, respectively (Bozza et al., 2002). The mOR-EG-GFP line was made using a transgene consisting of 3.0 kb upstream of the mOR-EG transcription start site followed by mOR-EG-IRES-gapEGFP (Oka et al., 2006). To record from isolated ORNs, the suction pipette technique was used, which has two distinct advantages over the whole-cell or perforated patch recording configuration, considering the questions

addressed in this study. First, the suction pipette technique is a loose-patch-on-cell recording configuration that does not perturb the intracellular milieu and also does not decrease the input resistance of ORNs. The whole-cell recording configuration can easily cause changes in basal firing in cells with such high input resistances as observed in ORNs. Second, spike firing of ORNs still located in the intact epithelium is modulated by neurotransmitters and hormones (Kawai et al., 1999; Savigner et al., 2009), thus making it difficult to unambiguously attribute changes in spike firing to OR-mediated events, which is not the case in isolated ORNs. I exposed mOR-EG, M71, or I7-expressing ORNs for 1 s to 100 µM eugenol, acetophenone, or heptanal (the mOR-EG, M71, and I7 ligands, respectively) (Krautwurst et al., 1998; Zhao et al., 1998; Kajiya et al., 2001; Bozza et al., 2002; Fig. 1, A–C). This elicited responses that were all near the maximal, saturating current (unpublished data) and displayed APs only during the rising phase of the receptor current as expected from near-saturating current responses (Reisert and Matthews, 2001a). In the absence of stimulation, mOR-EG ORNs showed very little basal spike firing activity (0.06 ± 0.02 Hz) in contrast to M71 and I7-expressing ORNs, which fired APs at an average frequency of 1.2 ± 0.6 and 1.9 ± 0.8 Hz (see Fig. 1, D–F, and Fig. 2 D for ana-

lyzed and averaged data and numbers of cells recorded). The increased spike activity was accompanied by an increase in receptor current fluctuations ("noise") in the M71 and I7-positive ORNs, which were absent in mOR-EG ORNs (Fig. 1, D−F, red traces; and on an expanded scale, see Fig. 1, G–H, to visualize the receptor current fluctuations). To investigate the source of the noise we used niflumic acid (300 µM), a blocker of the Ca^{2+}-activated Cl^- conductance (Kleene, 1993), which selectively reduces the Cl^- component of the odorant-induced receptor current by ∼80% but only weakly impacts the CNG channel current (Reisert et al., 2005). Basal AP activity and the current noise were abolished by blocking the Ca^{2+}-activated Cl^- conductance with niflumic acid (Fig. 1, D−F). This demonstrates that basal AP firing is driven by ciliary transduction events, as this is the localization of the Cl^- channel that is only present on the cilia and not the dendritic knob or dendrite (Stephan et al., 2009; Hengl et al., 2010; Rasche et al., 2010). Basal noise is not driven by, for example, mechanisms originating in the cell body, because niflumic acid was only supplied to the cilia and not the cell body, which resided inside the suction pipette. Interestingly this also indicates that the Cl^- conductance and its current are required to drive basal spike firing. CNG channel activity alone, which will trigger opening
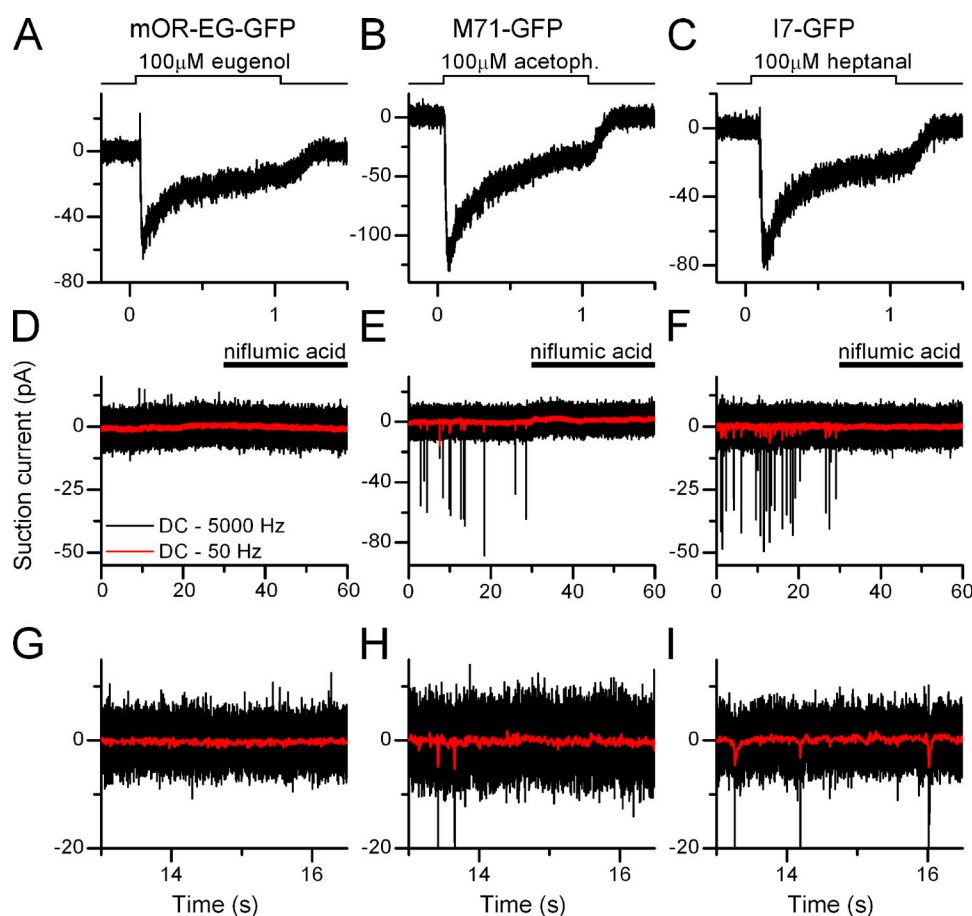

Figure 1. Basal action potential activity in olfactory receptor neurons. A–C show responses from isolated ORNs expressing the identified odorant receptors mOR-EG, M71, and I7 stimulated with their respective ligands eugenol, acetophenone, and heptanal. (D–F) Recordings in the absence of stimulation to monitor basal spike firing activity, same three cells as above. Red, low-pass (50 Hz) filtered recordings to display the underlying fluctuations of the receptor current. The Ca^{2+}-activated Cl^- channel blocker niflumic acid (300 µM, applied from 30 to 60 s) entirely abolished basal activity. (G–I) Expanded view of the same traces as in D–E to show current fluctuations.

of the Cl⁻ current but only carries a small current, is not sufficient.

To investigate the kinetics and frequency compositions of the current noise underlying the basal AP firing, power spectrum analysis was performed on current recordings filtered at DC-5000 Hz recorded in the absence of stimulation and in the presence of niflumic acid. The latter was done to obtain the baseline power spectrum, which depends on the seal resistance, instrumentation noise, and membrane channel noise not associated with the Cl⁻ channel. Little difference was observed in the basal and niflumic acid power spectra for mOR-EG recordings in agreement with the lack of noise and AP firing in the unstimulated recordings. In contrast, a large increase in power was observed in the 1–15-Hz frequency band derived from basal recordings above the niflumic acid power spectra in M71 and I7 ORNs (Fig. 2, A−C, black and blue traces are power spectra in the absence and presence of niflumic acid, respectively, 1–15 Hz frequency band shaded in gray).

The data were quantified by plotting the basal spike rate of different odorant receptor–expressing ORNs against the baseline current variance (Fig. 2 D). The variance (ΔVar) was calculated as the difference between the current variance in the absence and presence of niflumic acid (see Materials and methods) and represents a measure of the baseline noise. Basal spike rate was positively correlated with variance for the mOR-EG, M71, and I7 ORs. The mean spike rates are statistically different (one-way ANOVA, 0.05 level). A pairwise comparison (t test, 0.05 level) showed that spike rates for mOR-EG and M71 or I7 are also different. This suggests that, indeed, the OR choice sets and controls basal

noise levels and the basal firing rate. A concern is that the observed increase in noise and AP firing could potentially not originate from the I7 or M71 receptor, but from the coexpressed GFP. But because mOR-EG ORNs, which also express GFP, are not noisy, it seems unlikely that GFP is involved in noise generation either at the receptor level or other transduction components.

An explanation for the reduced level of noise in mOR-EG ORNs could be a reduced ability to generate current, for example, as a result of reduced transduction amplification or channel density. Determination of peak current responses elicited by 100 µM of the respective ligand revealed that mOR-EG, M71, and I7 ORNs all had comparable maximal current levels (within a factor of approximately two, see Fig. 2 E). Only mOR-EG and M71 current levels were statistically different (t test, 0.05 level). Maximal currents of the quiet mOR-EG ORNs and the noisy I7 ORNs were very comparable, suggesting that transduction downstream of the OR functions at equally efficient levels. Also, mOR-EG ORNs and the noisier M71 ORNs have similar EC_{50} for eugenol and acetophenone of 51 and 20 µM, respectively (Bozza et al., 2002; Oka et al., 2006), an indication that OR sensitivity and density might also not be grossly different.

As the three OR-GFP mice were of different genetic background, I investigated whether basal activity was determined by the mouse strain from which labeled ORNs were obtained. I repeated the above experiments using ORNs obtained from the I7-GFP mouse, which were randomly picked, not GFP positive, and responsive to the odorant cineole (100 µM, unpublished data). These cells showed a (statistically) significantly lower
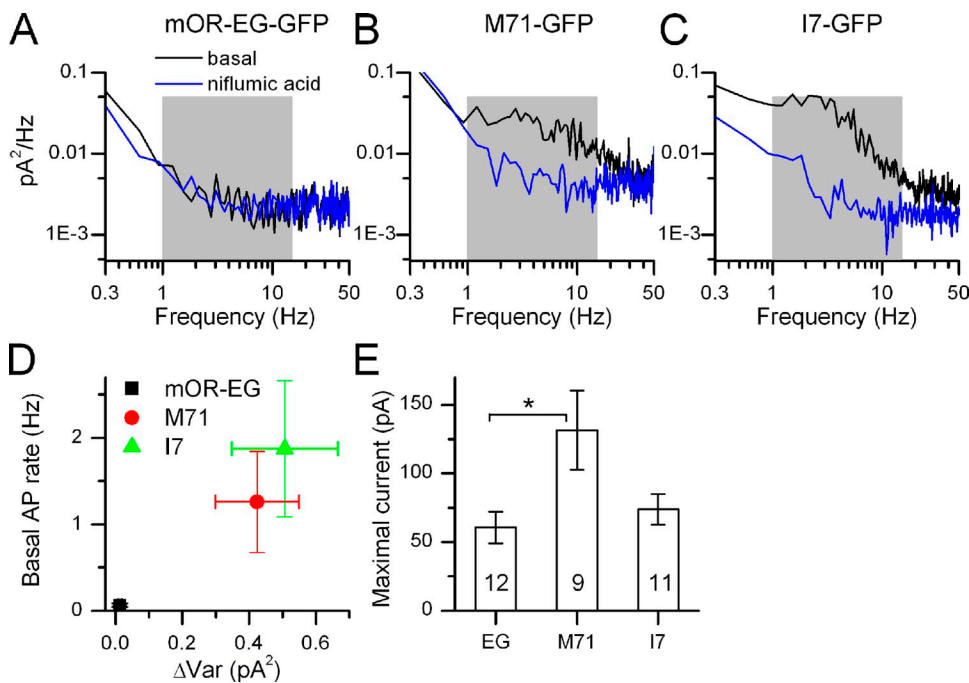

Figure 2. Kinetics of basal current fluctuations. (A–C) Power spectrum analysis of the black (filtered at DC-5000 Hz) traces in Fig. 1, D–F. Note the increase in noise in the 1–15-Hz band (shaded in gray) in the M71 and I7-positive ORNs, which is not observed in the mOR-EG–expressing ORN. (D) Average basal spike firing in the absence of stimulation as a function of basal variance (average of 9–12 ORNs). (E) Average maximal currents elicited by 100 µM of eugenol, acetophenone, and heptanal ORNs obtained from the mOR-EG, M71-GFP, and I7-GFP mouse lines, respectively. Numbers in the bars of the histograms are the numbers of cells recorded from. *, current levels that were statistically different (t test, 0.05 level). Data points are mean ± SEM.

basal AP firing activity (0.1 ± 0.03 Hz) and correspondingly low current noise levels (ΔVar = 0.06 ± 0.02 pA^2) compared with the noisy I7-GFP ORNs. Hence, noise levels and basal AP firing are not a property of a particular mouse strain, but again of individual ORNs expressing defined ORs.

As the level of noise seems to correlate with the specific receptor expressed in a given ORN, this suggests that it might be the receptor itself that leads to the generation of the increased noise. Basal, thermal activation of ORs will lead to activation of the transduction cascade and thus spontaneous small receptor currents, the level and frequency of which will depend on the individual receptors. If indeed the noise is generated by spontaneously activated ORs, one should be able to generate ("mimic") responses with similar time courses and frequency composition by exposing ORNs for short durations to odorants to activate ORs concurrently in a short time window. Ideally, stimulation would terminate before the odorant response begins such that all activated ORs contribute equally to the response (Bhandawat et al., 2005) before adaptational effects begin to contribute to the response kinetics. This can be achieved using fast solution changes (see Materials and methods) and thus (idealized) all ORs are activated at the same time.

I exposed I7-GFP ORNs to 0.3 µM heptanal for 30 ms to elicit a small response of similar size compared with those observed in the absence of stimulation (typically a few pico-amps, Fig. 3 A). The power spectrum derived from this response is shown in Fig. 3 B as is the spectrum obtained during application of niflumic acid (black and blue traces, respectively). The difference of those two spectra yields the power spectrum attributable

to the current carried by the Cl$^-$ channel (Fig. 3 C), which was fitted with the function $A_2 + (A_1 - A_2)/(1 + (f/f_0)^n)$, with A1 = 0.13 pA^{2}Hz^{-1}, A2 = 0.001 pA^{2}Hz^{-1}, f_0 = 6.4 Hz, and n = 3.4.

A similar analysis was performed for the basal transduction noise for the I7-expressing ORN in Fig. 1. The difference of the basal noise spectrum and the spectrum in the presence of niflumic acid was fitted with the above function to yield A1 = 0.04 pA^{2}Hz^{-1}, A2 = 0.001 pA^{2}Hz^{-1}, f_0 = 5.6 Hz, and n = 3.7 (Fig. 3 D). The parameter of most interest, f_0, since it describes the roll-off point of the power spectra and thus the frequency dependence of odorant-induced responses or basal activity, was 5.3 ± 0.5 Hz (n = 12) and 7.3 ± 1.1 Hz (n = 7), respectively (not statistically different, t test, 0.05 level). Four basal noise power spectra from I7 ORNs could not be fitted reliably due to a peak in the spectra around 6–7 Hz and were omitted from the analysis. Such peaks in the basal noise power spectra were never observed in the quieter mOR-EG or M71 ORNs and probably originated in the very high noise levels these particular four I7 ORNs displayed. Such high noise levels can begin to generate an additional standing current (as supposed to only random occasional current fluctuations), which in turn will lead to adaptation of the transduction mechanism and a change in response kinetics (Leinders-Zufall et al., 1999; Reisert and Matthews, 1999) and thus a change in power spectrum.

Fitting the basal noise power spectrum of M71 ORNs yielded f_0 = 7.1 ± 1.1 Hz (not statistically different from the two I7 values, t test, six cells; three more cells displayed noise levels too low to be fitted reliably), suggesting that the frequency composition of the basal noise is
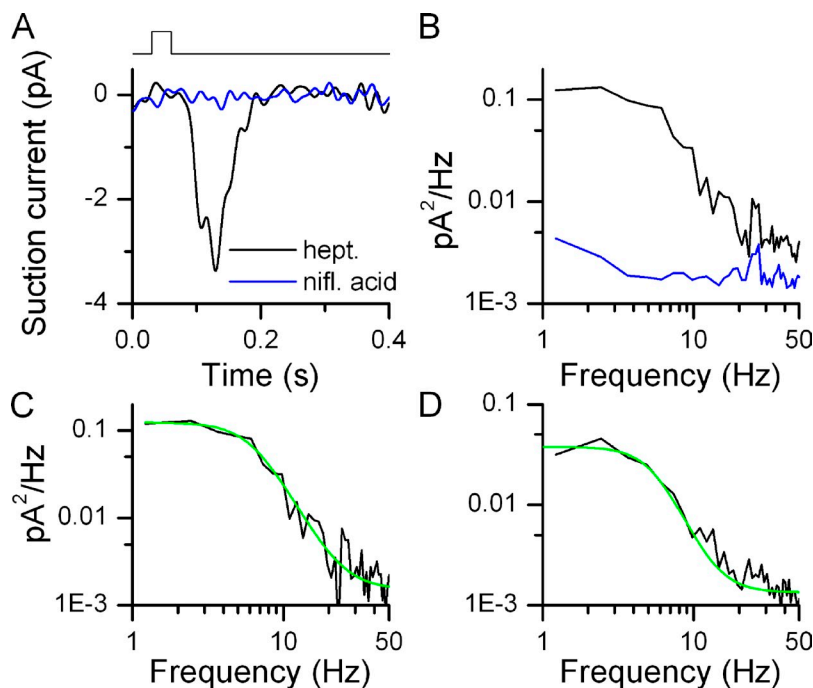

Figure 3. Kinetics of small odorant responses. (A) Suction pipette recordings from an I7-expressing ORN. Black trace is the average of 10 responses to 30-ms stimulations at 0.3 µM heptanal. Blue traces are the average of 10 recordings in the presence of 300 µM niflumic acid (no odorant) to suppress basal noise. The recording bandwidth of the displayed traces was 0–50 Hz. (B) Power spectrum analysis of corresponding traces (filtered at DC-5000 Hz) from A. Similar results in 12 ORNs. (C) Difference of the power spectra (odorant minus niflumic acid) in B fitted with $A_2 + (A_1 - A_2)/(1 + (f/f_0)^n)$, with A1 = 0.13 pA^{2}Hz^{-1}, A2 = 0.001 pA^{2}Hz^{-1}, f_0 = 6.4 Hz, and n = 3.4. (D) Difference of the power spectra (basal noise minus niflumic acid) in Fig. 2 C obtained from basal noise. Fitting parameters are A1 = 0.04 pA^{2}Hz^{-1}, A2 = 0.001 pA^{2}Hz^{-1}, f_0 = 5.6 Hz, and n = 3.7.

determined by transduction time constants other than the receptor lifetime, which is expected from the short dwell time of the odor molecule and the OR (Bhandawat et al., 2005). It might also suggest that a noise corner frequency around 6–7 Hz might be typical for all ORNs unless the basal OR activity is too high (see above). Other fitting parameters for M71 ORNs are $A1 = 0.08 \pm 0.02$ pA^{2}Hz^{-1}, $A2 = 0.002 \pm 0.001$ pA^{2}Hz^{-1}, and $n = 2.5 \pm 0.3$.

Collectively, OR stimulation elicits odorant responses with a time course similar to the basal noise and supports the notion that events that generate the noise are at the beginning of the transduction cascade driven by OR activity. Noise generated late in the transduction cascade by, for example, the two transduction channels is in the kHz range (Kleene, 1997), much higher than the frequency of around 5 Hz described here.

Control of basal cAMP levels and the odorant receptor

ORNs that express an odorant receptor with a high basal activity should also have a high basal ACIII rate even in the absence of stimulation because thermal OR activation will drive G protein and subsequently ACIII activation. Such basal ACIII activity can be uncovered by inhibiting cAMP degradation, and the application of IBMX, a phosphodiesterase blocker, should result in a large current. Conversely, ORNs should display little current in response to IBMX if the receptor protein has no basal activity, assuming that both the G protein and

ACIII have low basal activities themselves. This is indeed the case. We exposed mOR-EG, M71, and I7-expressing ORNs to eugenol, acetophenone, or heptanal (respectively at the saturating concentrations of 100 µM) and also 1 mM IBMX (Fig. 4). mOR-EG–positive ORNs only showed small responses at best when exposed to IBMX in contrast to I7-positive ORNs, which always showed a response. In response to IBMX, mOR-EG ORNs only generated currents $6 \pm 1\%$ of the eugenol response, whereas in I7-positive ORNs, a response of approximately half the size ($56 \pm 7\%$) of the odorant response was generated on average. M71 ORNs showed an intermediately sized response to IBMX ($21 \pm 6\%$).

The IBMX/odorant response ratio of different odorant receptor–expressing ORNs was plotted against the baseline current variance (Fig. 4 D). An increase in variance or baseline noise positively correlated with an increased IBMX response (statistically different at 0.005 level, one-way ANOVA) similar to the basal AP rate (see Fig. 2 D). Also, pairwise t tests (0.005 level) showed that the IBMX responses of mOR-EG, M71, and I7 ORNs are all different from each other. This suggests that the OR choice sets the level of basal ACIII activity.

Suppression of basal action potential firing by an inverse agonist

The source of the observed noise can be investigated in yet another direct way. I hypothesized that a receptor antagonist might not only prevent an agonist response
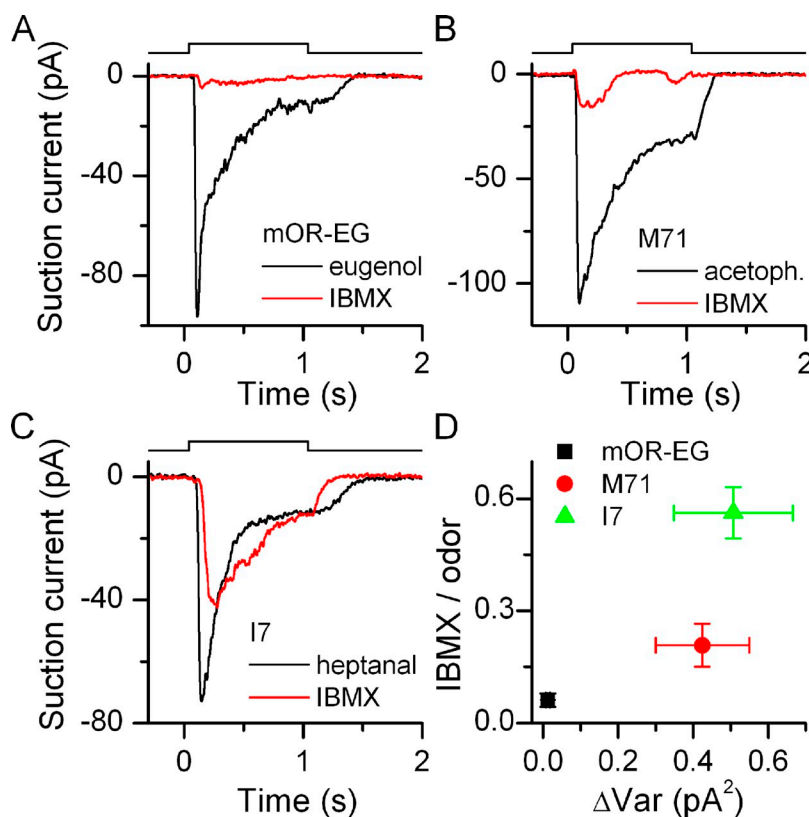

Figure 4. (A–C) The odorant receptor determines the response size to the phosphodiesterase inhibitor IBMX. mOR-EG, M71, and I7-expressing ORNs were exposed to their respective ligands at 100 µM and to 1 mM IBMX for 1 s. (D) For each ORN, the response to IBMX was normalized to their odorant response, average of 10–25 ORNs. Data points are mean ± SEM.

but also inhibit basal activity of the receptor, thus acting as an inverse agonist. Several antagonists for the I7 receptor have recently been published (Peterlin et al., 2008), and it was shown that increasing concentrations of the antagonists progressively reduced the Ca^{2+} signal obtained from an ORN that had been virally infected with the I7 OR and stimulated with 10 µM octanal. It has not been determined if the described antagonists can act as inverse agonists. Application of one of them, cycloheptanecarbaldehyde (chca), did indeed prevent basal spike firing (Fig. 5 A), making chca an inhibitory odorant. Chca also reduced the basal current noise in a
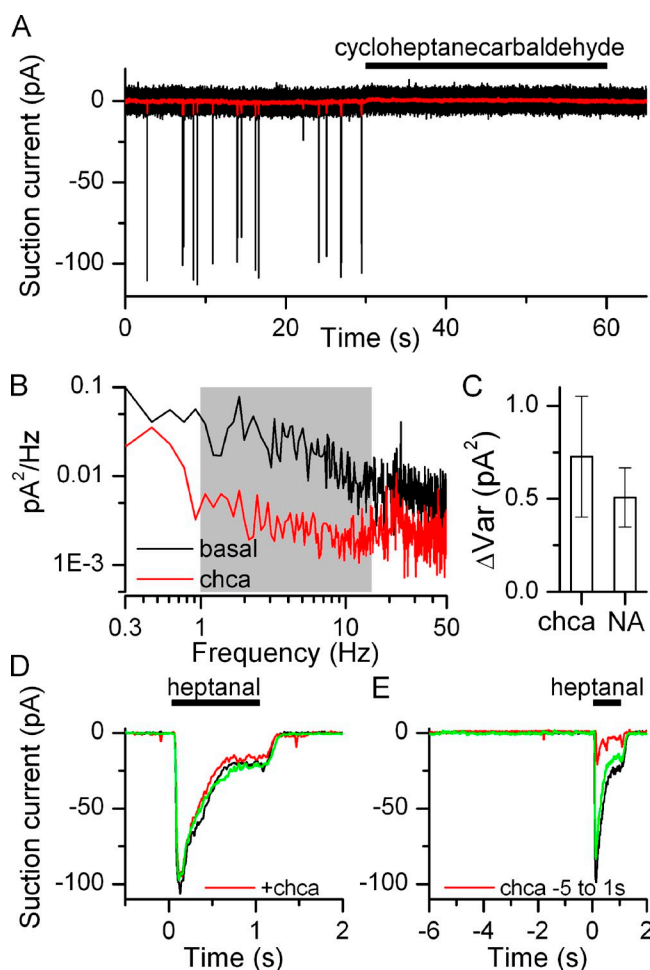
frequency-dependent manner similar to niflumic acid (Fig. 5 B), again in the 1–15-Hz frequency band (shaded in gray). Similar results were found in 14 ORNs. The ΔVar obtained from the chca application was not significantly different (*t* test) from the ΔVar obtained when suppressing basal activity with niflumic acid (Fig. 5 C).

A potential caveat is that chca might not only block the I7 receptor but also one of the transduction channels, as has been reported for other odorants (Takeuchi et al., 2009). This is not the case, because coapplication of heptanal and chca does not reduce the response to heptanal alone (Fig. 5 D). The average ratio of the heptanal + chca to the heptanal response was 1.004 ± 0.031 (not significantly different from 1, *t* test, $n = 16$), suggesting that chca has a lower affinity compared with heptanal. But chca can antagonize the heptanal-induced response, but only if the ORN is pre-exposed to chca (Fig. 5 E, average response ratio 0.48 ± 0.12, statistically different from 1 at 0.005 level, $n = 9$), potentially by being able to access the binding pocket before heptanal exposure. This heptanal response reduction after chca pre-exposure likely represents an underestimation because during the 5-s pre-exposure to chca, the ORN might recover from adaptation caused by the constant basal receptor activity and ensuing transduction noise. This can give rise to a potentially larger response when immediately stimulated after chca exposure. Together, these results suggest that indeed the observed noise is caused by basal odorant receptor activity and that chca is an inverse agonist for the I7 receptor.

The odorant receptor and the response pattern during prolonged stimulation

ORNs show quite distinct response patterns when stimulated for long durations. At intermediate odor concentrations, most ORNs show an oscillatory response pattern, firing bursts of APs at regular intervals, whereas some fire APs continuously. At high odorant concentrations, all ORNs, regardless of response pattern, saturate into a continuous receptor current (Reisert and Matthews, 2001a,b). ORNs expressing the odorant receptors mOR-EG, M71, and I7 were stimulated for 8 s with their respective ligands (Fig. 6 A). Both mOR-EG and I7-positive ORNs showed continuous activity after the initial large response at the onset of stimulation, whereas M71 ORNs showed an oscillatory response pattern. OR-specific response patterns for a given ORN were maintained over the intermediate concentration range (typically 3–10-fold) when ORNs were tested at more than one concentration. Similar results were obtained in 5–15 cells.

An autocorrelation analysis of the odorant-induced current was performed to find repeating and periodic patterns (Fig. 6 B). mOR-EG and I7 ORNs did not show clear peaks in their autocorrelogram, whereas M71 ORN did. All tested M71 ORNs showed clear oscillatory pattern, whereas this pattern was not observed in mOR-EG

Figure 5. Suppression of basal firing by an inverse agonist. (A) Suction pipette recordings of an I7-expressing ORN. Application of cycloheptanecarbaldehyde (chca, 100 µM), previously described as an I7 receptor antagonist (Peterlin et al., 2008), suppressed all basal firing. (B) Power spectra analysis in the absence and presence of chca, 1–15 Hz frequency band shaded in gray. (C) Suppression of noise (ΔVar) is similar with chca and niflumic acid (NA), mean ± SEM, $n = 14$ for chca and 11 for NA. (D) chca does not reduce the response when coapplied with heptanal (both odorants at 100 µM). Only preapplication (5 s) of the antagonist leads to response reduction. (E) Black and green traces are recorded before and after chca application. All recordings are from the same ORN.

or I7 ORNs ($n = 11$ and 14). The mean oscillation period (taken as the time of the first peak in the autocorelogram) for M71 ORNs was 0.57 ± 0.04 s (mean $\pm$ SEM, $n = 5$ ORNs, each tested at 1–3 acetophenone concentrations). Interestingly, randomly picked ORNs, which responded to cineole with an oscillatory response pattern, had a longer oscillation period of 1.4 ± 0.2 s (Reisert and Matthews, 2001a), but it remains to be seen if ORNs expressing other identified ORs have oscillation periods different from the one reported here for M71-expressing ORNs. Additionally, we previously investigated response patterns during prolonged stimulation in great detail in frog ORNs (Reisert and Matthews, 2001b), and to a lesser extent in mouse ORNs (Reisert and Matthews, 2001a), and demonstrated that randomly picked ORNs expressing random ORs stimulated with the odorant cineole can display three distinctive response patterns: "silent" (no further response after a transient response at the onset of stimulation), "oscillatory" (as seen in M71 ORNs), and "continuous" (as seen in I7 and mOR-EG ORNs). This suggests that the response pattern

is not a property of the odorant, but more probably of the stimulated ORN expressing a particular OR. The precise mechanism that determines response patterns remains to be elucidated, but it is interesting to note that the class of ORNs that showed an oscillatory response pattern (M71 ORNs) have larger, although not always statistically different, transduction currents (Fig. 2 E), which might be required to drive ORNs into oscillations.

In conclusion, the odorant receptor is likely to contribute to, and control the response pattern during, long stimulation periods, but the precise mechanism that sets response mode and oscillation period remains to be investigated.

DISCUSSION

Response properties of mouse odorant receptor neurons with identified odorant receptors

Understanding the contribution of mammalian odorant receptors to the odorant-induced response has focused on elucidating the response profiles and ligand sensitivity of ORs. Deorphanization of ORs has seen substantial progress (for example see Saito et al., 2009), but OR properties, other than ligand specificity, that might contribute to the odorant-induced response, have not been addressed. This work investigated the source of basal action potential frequency and current noise in ORNs.

I characterized three mouse lines, which express GFP with the mOR-EG, M71 or I7 OR for identification, with respect to their ORNs' basal AP rate, current noise levels, and response patterns. ORNs expressing a given, identified receptor had different basal noise levels that correlated positively with basal AP rates (Figs. 1 and 2). Both noise levels and basal AP rates depend on transduction activity and current carried by the olfactory Ca^{2+}-activated Cl^{-} channel. CNG channel activity alone is not sufficient to drive basal AP activity. This demonstrates that in mammalian ORNs, even at low level of activity, the amplification of the CNG current by the Cl^{-} channel is required.

Basal noise could have its origin in a high basal G protein or ACIII activity (without basal OR activity) or high spontaneous opening of the CNG and Cl^{-} channel. This seems unlikely since, first, the response to the phosphodiesterase inhibitor IBMX, which monitors basal ACIII activity, correlated with basal noise and OR (Fig. 4). This implicates the OR as the origin of the current noise. Additionally mOR-EG ORNs (and also randomly picked cineole-responsive ORNs, which probably will have expressed several different ORs) show very low basal activity, which demonstrates that both G protein and ACIII have a low constitutive activity, a prerequisite to prime ORNs to be sensitive to the level of basal OR activity.
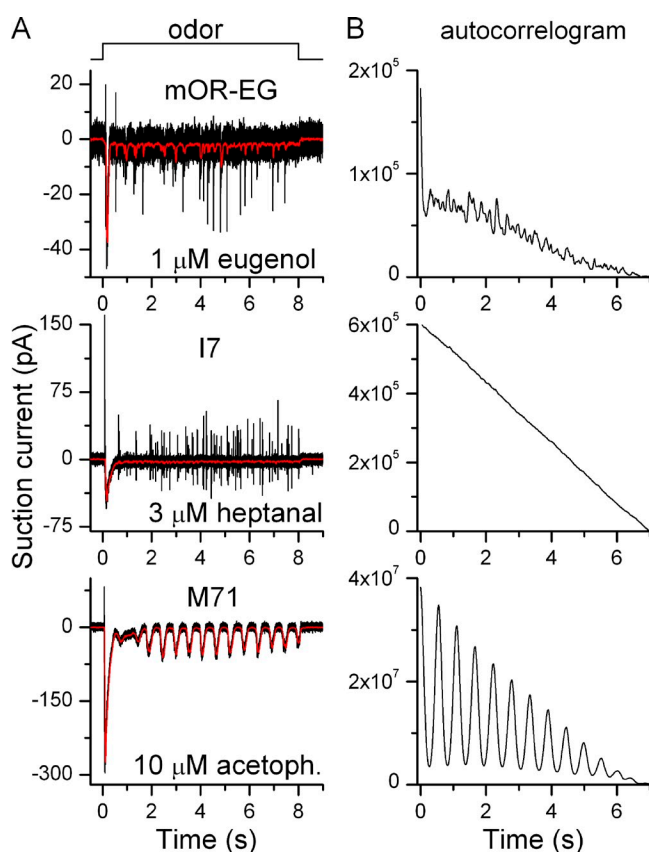

Figure 6. The odorant receptor determines response patterns during prolonged stimulation. (A) mOR-EG, M71, and I7-expressing ORNs were exposed to their respective ligands for 8 s at concentrations indicated next to each trace. Black and red recordings were filtered at DC-5000 Hz and DC-50 Hz, respectively. (B) The traces in A were auto-correlogrammed from 1–8 s to reveal underlying preferred response periodicities.

Second, the power spectrum of the basal noise (Fig. 1 and 2) of I7 and M71 ORNs displayed a cut-off at around 7 Hz, a frequency much lower than the noise generated by channel openings of the CNG and Cl^- channel, which is around 1000 Hz (Kleene, 1997). Furthermore, power spectra of small I7-expressing ORN responses evoked by short stimulations (Fig. 2) to mimic spontaneous activity showed a similar cut-off frequency, again implicating OR activity as the driving source of basal noise. Interestingly, the frequency band up to 7 Hz, which describes these responses, is similar to the breathing frequency of mice and rats (Youngentob et al., 1987; Tankersley et al., 1994; Kepecs et al., 2007; Wesson et al., 2008), suggesting that ORN signal transduction might be "tuned" to match the stimulation frequency imposed by rhythmic odorant delivery during breathing or sniffing.

The origin of transduction noise and the resulting receptor current noise have been thoroughly investigated in another sensory, G protein–coupled system: vision. In rod photoreceptors, two main sources of noise have been identified: a discrete slow component with a time course of around 1 s (caused by spontaneous activation of a single rhodopsin and thus the entire transduction cascade) and a fast continuous noise (attributed to spontaneous downstream phosphodiesterase activity) (Baylor et al., 1980; Rieke and Baylor, 1996).

Does the current noise observed in ORNs represent the lifetime of a single activated OR as is the case with rhodopsin in photoreceptors? This is probably not the case because the lifetime of a ligand-activated OR is of the order of 1 ms, much faster than the responses observed (Bhandawat et al., 2005). These observations are consistent with the response kinetics being dominated by the lifetime of downstream components, e.g., the G protein–ACIII complex or PDE1C and Na^+/Ca^{2+} exchanger kinetics. Additionally, with the response of a single activated OR being very small (<0.02 pA in frog ORNs; Bhandawat et al., 2005), the observed noise fluctuations, which can reach a few pico-amps, will stem from many simultaneously activated ORs. Underlying assumptions here are that the lifetime of a ligand-bound OR is similar to a spontaneously activated OR, that OR–G protein coupling is similar in either case and that G protein coupling is similar across different ORs. Another open question is whether a spontaneously active OR can also lead to changes in the expression level of other signal transduction components, although such effects seem to be limited in magnitude (Fig. 2 E).

Basal activity, inhibitory responses, and inverse agonists
Inhibitory responses to odorants have been reported in the form of a reduction in basal firing, the generation of a hyperpolarizing receptor current, or the suppression of an excitatory odorant-induced inward current (O'Connell and Mozell, 1969; Getchell and Shepherd,

1978; Kurahashi et al., 1994; Morales et al., 1994). Mechanisms mediating inhibitory responses include blockage of the CNG channel by odorants or activation of Ca^{2+}-activated K^+ channels (Morales et al., 1994; Takeuchi et al., 2009). As I show here, the (I7) OR itself can mediate an inhibitory response by suppression of basal activity by an inverse agonist. But as not all ORs display basal activity, only a defined subset of ORs will be susceptible to reducing basal activity via an inverse agonist. Such suppression might be significant at the level of the olfactory bulb due to the high convergence of ~1,000 ORNs onto a single glomerulus and the high "set point" of basal activity of second order neurons in the olfactory bulb in vivo in awake behaving mice (Rinberg et al., 2006). An interesting observation was that randomly chosen ORNs with different unknown ORs that responded to cineole showed little basal activity on average. This suggests that certain odorants may have an affinity for ORs with low basal activity.

In an interesting parallel, inverse agonism is exemplified in a closely related GPCR, the visual pigment rhodopsin. 11-cis retinal binds covalently to rod opsin in its binding pocket to suppress nearly all basal activity of free opsin and subsequent activation of the phototransduction cascade. This suppression, combined with a low thermal activation rate, contributes to the high sensitivity and amplification of rod photoreceptors (Fain et al., 2001; Lamb and Pugh, 2004). In contrast, cone pigment can have a much higher spontaneous isomerization rate in darkness and thus can display higher levels of basal activity and transduction current, rendering cones less light sensitive than rods (Rieke and Baylor, 2000; Kefalov et al., 2003).

The odorant receptor and targeting
Targeting of axons along the bulbar anteroposterior axis is mediated by an unknown mechanism that depends on differential $G_{\alpha s}$ and ACIII activity (Imai et al., 2006; Chesler et al., 2007). Could the observed varying basal, thermal activity of individual ORs play a role or even be a determinate in targeting ORN axons to glomeruli in the bulb? In such a scenario, increased basal OR activity should lead to $G_{\alpha s}$ and ACIII activity, and thus ORs with higher basal activity should target to glomeruli located progressively posteriorly. For the three ORs for which I determined the basal activity, the glomeruli of the most quiet OR (mOR-EG) are indeed located anteriorally, and the M71 glomeruli (intermediate basal activity) are positioned at the posterior end of the bulb (Bozza et al., 2002; Oka et al., 2006). The rat I7 OR (which differs from the mouse OR in only 15 amino acids) when expressed in the M71 locus, targets intermediately along the anteroposterior axis, thus not as posteriorly as one would expect based on basal activity compared with M71. This assumes that the rat I7 OR has the same basal activity compared with its mouse

counterpart. That rat I7 has at least some basal activity is supported by the observation that manipulations designed to decrease cAMP levels in ORNs expressing rat I7 cause an anterior shift of the I7 glomerulus (Imai et al., 2006). Similarly, a mouse that is hypomorphic for M71, and that might therefore have reduced levels of basal OR activity, has anteriorly shifted glomeruli (Feinstein et al., 2004). The β2 (but not the β1 adrenergic) adrenergic receptor displays basal activity when expressed in cardiac myocytes (Zhou et al., 2000), and the glomerulus innervated by β2 adrenergic receptor–positive ORNs is located not anteriorly but midway along the anteroposterior axis (Feinstein et al., 2004).

Although the scenario of basal OR activity as a contributor to anteroposterior glomerular map formation might be simple and elegant, these results should be interpreted with some caution. I determined the basal activity of ORs located on the cilia of mature ORNs coupled to $G_{\alpha olf}$, which might be quite different from the basal activity of the same receptors in the environment of an immature ORN coupled to $G_{\alpha s}$ located in, for example, the growth cone expressed at a different density. Basal OR activity might also be different in a heterologous system. Additionally, other mechanisms contribute to dorsal–ventral glomerular location, which roughly follows the zonal OR expression arrangement in the olfactory epithelium (Feinstein and Mombaerts, 2004; Miyamichi et al., 2005) or cellular identity (Bozza et al., 2009). Local sorting of axons once they reached their position along the anteroposterior axis has been proposed to be dependent on extrinsic (odor)-mediated activity (Serizawa et al., 2006). The contribution of basally active ORs and increased basal activity to this mechanism remains unclear.

The link between basal activation of GPCRs and crystal structure could be investigated in the β adrenoreceptors and rhodopsin. It is thought to arise partly from the polar interaction between a conserved DRY motif on TM3 and a glutamate residue on TM6, which is broken in the ligand-activated GPCRs (Rosenbaum et al., 2009). Unfortunately, the crystal structure for even one OR is not available, limiting structural comparisons with other GPCRs. But the modeling and experimental validation of odorant–OR interactions have made significant progress over the recent years (for review see Reisert and Restrepo, 2009). Incorporating basal activity of native and genetically modified ORs might become feasible. This should yield a more detailed understanding of ORs and their contribution to the response properties of ORNs and their axon targeting.

REFERENCES

Baylor, D.A., G. Matthews, and K.W. Yau. 1980. Two components of electrical dark noise in toad retinal rod outer segments. *J. Physiol.* 309:591–621.

Bhandawat, V., J. Reisert, and K.W. Yau. 2005. Elementary response of olfactory receptor neurons to odorants. *Science.* 308:1931–1934. doi:10.1126/science.1109886

Bozza, T., P. Feinstein, C. Zheng, and P. Mombaerts. 2002. Odorant receptor expression defines functional units in the mouse olfactory system. *J. Neurosci.* 22:3033–3043.

Bozza, T., A. Vassalli, S. Fuss, J.J. Zhang, B. Weiland, R. Pacifico, P. Feinstein, and P. Mombaerts. 2009. Mapping of class I and class II odorant receptors to glomerular domains by two distinct types of olfactory sensory neurons in the mouse. *Neuron.* 61:220–233. doi:10.1016/j.neuron.2008.11.010

Chesler, A.T., D.J. Zou, C.E. Le Pichon, Z.A. Peterlin, G.A. Matthews, X. Pei, M.C. Miller, and S. Firestein. 2007. A G protein/cAMP signal cascade is required for axonal convergence into olfactory glomeruli. *Proc. Natl. Acad. Sci. USA.* 104:1039–1044. doi:10.1073/pnas.0609215104

Cygnar, K.D., and H. Zhao. 2009. Phosphodiesterase 1C is dispensable for rapid response termination of olfactory sensory neurons. *Nat. Neurosci.* 12:454–462. doi:10.1038/nn.2289

Dahanukar, A., E.A. Hallem, and J.R. Carlson. 2005. Insect chemoreception. *Curr. Opin. Neurobiol.* 15:423–430. doi:10.1016/j.conb.2005.06.001

Fain, G.L., H.R. Matthews, M.C. Cornwall, and Y. Koutalos. 2001. Adaptation in vertebrate photoreceptors. *Physiol. Rev.* 81:117–151.

Feinstein, P., and P. Mombaerts. 2004. A contextual model for axonal sorting into glomeruli in the mouse olfactory system. *Cell.* 117:817–831. doi:10.1016/j.cell.2004.05.011

Feinstein, P., T. Bozza, I. Rodriguez, A. Vassalli, and P. Mombaerts. 2004. Axon guidance of mouse olfactory sensory neurons by odorant receptors and the beta2 adrenergic receptor. *Cell.* 117:833–846. doi:10.1016/j.cell.2004.05.013

Fleischer, J., H. Breer, and J. Strotmann. 2009. Mammalian olfactory receptors. *Front. Cell. Neurosci.* 3:9. doi:10.3389/neuro.03.009.2009

Frings, S., S. Benz, and B. Lindemann. 1991. Current recording from sensory cilia of olfactory receptor cells *in situ.* 2. Role of mucosal Na$^+$, K$^+$, and Ca^{2+} ions. *J. Gen. Physiol.* 97:725–747. doi:10.1085/jgp.97.4.725

Getchell, T.V., and G.M. Shepherd. 1978. Adaptive properties of olfactory receptors analysed with odour pulses of varying durations. *J. Physiol.* 282:541–560.

Grosmaitre, X., A. Vassalli, P. Mombaerts, G.M. Shepherd, and M. Ma. 2006. Odorant responses of olfactory sensory neurons expressing the odorant receptor MOR23: a patch clamp analysis in gene-targeted mice. *Proc. Natl. Acad. Sci. USA.* 103:1970–1975. doi:10.1073/pnas.0508491103

Hengl, T., H. Kaneko, K. Dauner, K. Vocke, S. Frings, and F. Möhrlen. 2010. Molecular components of signal amplification in olfactory sensory cilia. *Proc. Natl. Acad. Sci. USA.* 107:6052–6057. doi:10.1073/pnas.0909032107

Imai, T., and H. Sakano. 2008. Odorant receptor-mediated signaling in the mouse. *Curr. Opin. Neurobiol.* 18:251–260. doi:10.1016/j.conb.2008.07.009

Imai, T., M. Suzuki, and H. Sakano. 2006. Odorant receptor–derived cAMP signals direct axonal targeting. *Science.* 314:657–661. doi:10.1126/science.1131794

Kajiya, K., K. Inaki, M. Tanaka, T. Haga, H. Kataoka, and K. Touhara. 2001. Molecular bases of odor discrimination: reconstitution of olfactory receptors that recognize overlapping sets of odorants. *J. Neurosci.* 21:6018–6025.

Kato, A., and K. Touhara. 2009. Mammalian olfactory receptors: pharmacology, G protein coupling and desensitization. *Cell. Mol. Life Sci.* 66:3743–3753. doi:10.1007/s00018-009-0111-6

Kaupp, U.B. 2010. Olfactory signalling in vertebrates and insects: differences and commonalities. *Nat. Rev. Neurosci.* 11:188–200.

Kawai, F., T. Kurahashi, and A. Kaneko. 1999. Adrenaline enhances odorant contrast by modulating signal encoding in olfactory receptor cells. *Nat. Neurosci.* 2:133–138. doi:10.1038/5686

Kefalov, V., Y. Fu, N. Marsh-Armstrong, and K.W. Yau. 2003. Role of visual pigment properties in rod and cone phototransduction. *Nature.* 425:526–531. doi:10.1038/nature01992

Kepecs, A., N. Uchida, and Z.F. Mainen. 2007. Rapid and precise control of sniffing during olfactory discrimination in rats. *J. Neurophysiol.* 98:205–213. doi:10.1152/jn.00071.2007

Kleene, S.J. 1993. Origin of the chloride current in olfactory transduction. *Neuron.* 11:123–132. doi:10.1016/0896-6273(93)90276-W

Kleene, S.J. 1997. High-gain, low-noise amplification in olfactory transduction. *Biophys. J.* 73:1110–1117. doi:10.1016/S0006-3495(97)78143-8

Kleene, S.J. 2008. The electrochemical basis of odor transduction in vertebrate olfactory cilia. *Chem. Senses.* 33:839–859. doi:10.1093/chemse/bjn048

Krautwurst, D., K.W. Yau, and R.R. Reed. 1998. Identification of ligands for olfactory receptors by functional expression of a receptor library. *Cell.* 95:917–926. doi:10.1016/S0092-8674(00)81716-X

Kurahashi, T., and K.-W. Yau. 1993. Co-existence of cationic and chloride components in odorant-induced current of vertebrate olfactory receptor cells. *Nature.* 363:71–74. doi:10.1038/363071a0

Kurahashi, T., G. Lowe, and G.H. Gold. 1994. Suppression of odorant responses by odorants in olfactory receptor cells. *Science.* 265:118–120. doi:10.1126/science.8016645

Lamb, T.D., and E.N. Pugh Jr. 2004. Dark adaptation and the retinoid cycle of vision. *Prog. Retin. Eye Res.* 23:307–380. doi:10.1016/j.preteyeres.2004.03.001

Leinders-Zufall, T., M. Ma, and F. Zufall. 1999. Impaired odor adaptation in olfactory receptor neurons after inhibition of Ca^{2+}/calmodulin kinase II. *J. Neurosci.* 19:RC19.

Lowe, G., and G.H. Gold. 1991. The spatial distributions of odorant sensitivity and odorant-induced currents in salamander olfactory receptor cells. *J. Physiol.* 442:147–168.

Lowe, G., and G.H. Gold. 1993. Nonlinear amplification by calcium-dependent chloride channels in olfactory receptor cells. *Nature.* 366:283–286. doi:10.1038/366283a0

Lowe, G., and G.H. Gold. 1995. Olfactory transduction is intrinsically noisy. *Proc. Natl. Acad. Sci. USA.* 92:7864–7868. doi:10.1073/pnas.92.17.7864

Malnic, B. 2007. Searching for the ligands of odorant receptors. *Mol. Neurobiol.* 35:175–181. doi:10.1007/s12035-007-0013-2

Matthews, H.R. 1999. A compact modular flow heater for the superfusion of mammalian cells. *J. Physiol. (Lond.)* 518:13P. doi:10.1111/j.1469-7793.1999.0867p.x

Miyamichi, K., S. Serizawa, H.M. Kimura, and H. Sakano. 2005. Continuous and overlapping expression domains of odorant receptor genes in the olfactory epithelium determine the dorsal/ventral positioning of glomeruli in the olfactory bulb. *J. Neurosci.* 25:3586–3592. doi:10.1523/JNEUROSCI.0324-05.2005

Mombaerts, P. 2004. Genes and ligands for odorant, vomeronasal and taste receptors. *Nat. Rev. Neurosci.* 5:263–278. doi:10.1038/nrn1365

Mombaerts, P. 2006. Axonal wiring in the mouse olfactory system. *Annu. Rev. Cell Dev. Biol.* 22:713–737. doi:10.1146/annurev.cellbio.21.012804.093915

Morales, B., G. Ugarte, P. Labarca, and J. Bacigalupo. 1994. Inhibitory K^+ current activated by odorants in toad olfactory neurons. *Proc. Biol. Sci.* 257:235–242. doi:10.1098/rspb.1994.0120

Munger, S.D., T. Leinders-Zufall, and F. Zufall. 2009. Subsystem organization of the mammalian sense of smell. *Annu. Rev. Physiol.* 71:115–140. doi:10.1146/annurev.physiol.70.113006.100608

O'Connell, R.J., and M.M. Mozell. 1969. Quantitative stimulation of frog olfactory receptors. *J. Neurophysiol.* 32:51–63.

Oka, Y., S. Katada, M. Omura, M. Suwa, Y. Yoshihara, and K. Touhara. 2006. Odorant receptor map in the mouse olfactory bulb: in vivo sensitivity and specificity of receptor-defined glomeruli. *Neuron.* 52:857–869. doi:10.1016/j.neuron.2006.10.019

Peterlin, Z., Y. Li, G. Sun, R. Shah, S. Firestein, and K. Ryan. 2008. The importance of odorant conformation to the binding and activation of a representative olfactory receptor. *Chem. Biol.* 15:1317–1327. doi:10.1016/j.chembiol.2008.10.014

Rasche, S., B. Toetter, J. Adler, A. Tschapek, J.F. Doerner, S. Kurtenbach, H. Hatt, H. Meyer, B. Warscheid, and E.M. Neuhaus. 2010. Tmem16b is specifically expressed in the cilia of olfactory sensory neurons. *Chem. Senses.* 35:239–245. doi:10.1093/chemse/bjq007

Reisert, J., and H.R. Matthews. 1999. Adaptation of the odour-induced response in frog olfactory receptor cells. *J. Physiol.* 519:801–813. doi:10.1111/j.1469-7793.1999.0801n.x

Reisert, J., and H.R. Matthews. 2001a. Response properties of isolated mouse olfactory receptor cells. *J. Physiol.* 530:113–122. doi:10.1111/j.1469-7793.2001.0113m.x

Reisert, J., and H.R. Matthews. 2001b. Responses to prolonged odour stimulation in frog olfactory receptor cells. *J. Physiol.* 534:179–191. doi:10.1111/j.1469-7793.2001.t01-1-00179.x

Reisert, J., and D. Restrepo. 2009. Molecular tuning of odorant receptors and its implication for odor signal processing. *Chem. Senses.* 34:535–545. doi:10.1093/chemse/bjp028

Reisert, J., J. Lai, K.W. Yau, and J. Bradley. 2005. Mechanism of the excitatory Cl^- response in mouse olfactory receptor neurons. *Neuron.* 45:553–561. doi:10.1016/j.neuron.2005.01.012

Rieke, F., and D.A. Baylor. 1996. Molecular origin of continuous dark noise in rod photoreceptors. *Biophys. J.* 71:2553–2572. doi:10.1016/S0006-3495(96)79448-1

Rieke, F., and D.A. Baylor. 2000. Origin and functional impact of dark noise in retinal cones. *Neuron.* 26:181–186. doi:10.1016/S0896-6273(00)81148-4

Rinberg, D., A. Koulakov, and A. Gelperin. 2006. Sparse odor coding in awake behaving mice. *J. Neurosci.* 26:8857–8865. doi:10.1523/JNEUROSCI.0884-06.2006

Rosenbaum, D.M., S.G. Rasmussen, and B.K. Kobilka. 2009. The structure and function of G-protein-coupled receptors. *Nature.* 459:356–363. doi:10.1038/nature08144

Saito, H., Q. Chi, H. Zhuang, H. Matsunami, and J.D. Mainland. 2009. Odor coding by a Mammalian receptor repertoire. *Sci. Signal.* 2:ra9. doi:10.1126/scisignal.2000016

Savigner, A., P. Duchamp-Viret, X. Grosmaitre, M. Chaput, S. Garcia, M. Ma, and B. Palouzier-Paulignan. 2009. Modulation of spontaneous and odorant-evoked activity of rat olfactory sensory neurons by two anorectic peptides, insulin and leptin. *J. Neurophysiol.* 101:2898–2906. doi:10.1152/jn.91169.2008

Serizawa, S., K. Miyamichi, H. Takeuchi, Y. Yamagishi, M. Suzuki, and H. Sakano. 2006. A neuronal identity code for the odorant receptor-specific and activity-dependent axon sorting. *Cell.* 127:1057–1069. doi:10.1016/j.cell.2006.10.031

Spehr, M., and S.D. Munger. 2009. Olfactory receptors: G protein-coupled receptors and beyond. *J. Neurochem.* 109:1570–1583. doi:10.1111/j.1471-4159.2009.06085.x

Stephan, A.B., E.Y. Shum, S. Hirsh, K.D. Cygnar, J. Reisert, and H. Zhao. 2009. ANO2 is the cilial calcium-activated chloride channel that may mediate olfactory amplification. *Proc. Natl. Acad. Sci. USA.* 106:11776–11781. doi:10.1073/pnas.0903304106

Su, C.Y., K. Menuz, and J.R. Carlson. 2009. Olfactory perception: receptors, cells, and circuits. *Cell.* 139:45–59. doi:10.1016/j.cell.2009.09.015

Takeuchi, H., H. Ishida, S. Hikichi, and T. Kurahashi. 2009. Mechanism of olfactory masking in the sensory cilia. *J. Gen. Physiol.* 133:583–601. doi:10.1085/jgp.200810085

Tankersley, C.G., R.S. Fitzgerald, and S.R. Kleeberger. 1994. Differential control of ventilation among inbred strains of mice. *Am. J. Physiol.* 267:R1371–R1377.

Trotier, D., and P. MacLeod. 1983. Intracellular recordings from salamander olfactory receptor cells. *Brain Res.* 268:225–237. doi:10.1016/0006-8993(83)90488-2

Wesson, D.W., T.N. Donahou, M.O. Johnson, and M. Wachowiak. 2008. Sniffing behavior of mice during performance in odor-guided tasks. *Chem. Senses.* 33:581–596. doi:10.1093/chemse/bjn029

Youngentob, S.L., M.M. Mozell, P.R. Sheehe, and D.E. Hornung. 1987. A quantitative analysis of sniffing strategies in rats performing odor detection tasks. *Physiol. Behav.* 41:59–69. doi:10.1016/0031-9384(87)90131-4

Zhao, H., L. Ivic, J.M. Otaki, M. Hashimoto, K. Mikoshiba, and S. Firestein. 1998. Functional expression of a mammalian odorant receptor. *Science.* 279:237–242. doi:10.1126/science.279.5348.237

Zhou, Y.Y., D. Yang, W.Z. Zhu, S.J. Zhang, D.J. Wang, D.K. Rohrer, E. Devic, B.K. Kobilka, E.G. Lakatta, H. Cheng, and R.P. Xiao. 2000. Spontaneous activation of beta(2)- but not beta(1)-adrenoceptors expressed in cardiac myocytes from beta(1)beta(2) double knockout mice. *Mol. Pharmacol.* 58:887–894.

Zou, D.J., A. Chesler, and S. Firestein. 2009. How the olfactory bulb got its glomeruli: a just so story? *Nat. Rev. Neurosci.* 10:611–618. doi:10.1038/nrn2666